RT&A, No 4 (89)
Volume 20, December 2025

XAI-SPCNET: A MULTI-LEVEL EXPLAINABLE AI FRAMEWORK FOR PREDICTIVE CONTROL CHART AUTOMATION IN MANUFACTURING QUALITY MONITORING PROCESS

V. Anusha[1], Lilly George[1], K.S. Harish[2], Yuvaraja B[3], A. Manimaran[3*]

•

[1]Department of Statistics, St. Joseph's College, Bharathidasan University, Tiruchirapally, Tamil Nadu, India

[2]Department of data science, SIva Sivani Institute of Management, Secunderabad, Telangana, India

[3]Department of Mathematics, School of Advanced Sciences VIT-AP University, Amaravati, Andhra Pradesh, India

anushavemula189@gmail.com, lgaceg@gmail.com, drksharish@gmail.com, yuvarajaboddu1988@gmail.com, manimaran.a@vitap.ac.in*

Abstract

Timely and accurate detection of process abnormalities in modern manufacturing is needed for sustainable quality assurance so that the process can be rectified quickly. Traditional control charts, although good at illustrating deviations, are poor in prediction and heavily dependent on fixed thresholds, which tend to lead to tardy interventions and high rates of false alarms. Recent developments in artificial intelligence (AI) offer predictive options; nonetheless, their lack of transparency as "black-box" systems erodes users' confidence and influences regulatory compliance difficulties. To bridge this void, Explainable AI (XAI) is ever more critical for Statistical Process Control (SPC), delivering not just precise anomaly prediction but also interpretable, transparent explanations. This paper presents XAI-SPCNet, a new framework incorporating explainability into predictive SPC to facilitate better manufacturing quality assurance. The architecture involves several expert-informed components: (1) Temporal Causal Decision Trees (TCDT-SPE) using Granger causality for adaptive causal splits that are interpretable; (2) Dynamic Rule Embedding Networks (DREN) combining temporal embeddings with Bayesian rule learning for succinct, context-dependent rules; (3) Contrastive Explanation Generator (CEG-SPE) offering contrastive explanations for violations; (4) Sparse Symbolic Regression (SSR-ED) obtaining sparse mathematical decision boundaries; and (5) Multi-Objective Reinforcement Learner with Explanation Optimization (MORLEO) optimizing accuracy, truthfulness, and chart stability. In synthetic and real-world datasets, XAI-SPCNet presents high prediction accuracy (91%), fast inference, concise rule representation, and greater than 95% explanation coverage, thereby promoting transparent, adaptive, and reliable quality control in manufacturing.

Keywords: Explainable AI, Statistical Process Control, Predictive Quality Monitoring, Symbolic Regression, Reinforcement Learning, Process

DOI: https://doi.org/10.24412/1932-2321-2025-489-381-398

Table 1: *List of Abbreviations and Their Full Forms*

Abbreviation	Full Form
SPC	Statistical Process Control
ML	Machine Learning
AI	Artificial Intelligence
QC	Quality Control
ECG	Electrocardiogram
WAAM	Wire Arc Additive Manufacturing
AEWMA	Adaptive Exponentially Weighted Moving Average
RPA	Robotic Process Automation
WOA	Whale Optimization Algorithm
DBN	Deep Belief Network
OCT	Optical Coherence Tomography
ConvBiGRU	Convolutional Bidirectional Gated Recurrent Unit
RNN	Recurrent Neural Network
GAN	Generative Adversarial Network
AFP	Automated Fiber Placement
GMAW	Gas Metal Arc Welding
LWM	Laser Welding Monitoring
CAM	Computer-Aided Manufacturing
RUL	Remaining Useful Life
PCA	Principal Component Analysis
AE	Acoustic Emission
IoT	Internet of Things
BIM	Building Information Modeling
FEM	Finite Element Method
API	Application Programming Interface
UAV	Unmanned Aerial Vehicle
HMI	Human-Machine Interface
BMS	Bridge Management System
SNR	Signal-to-Noise Ratio
KPI	Key Performance Indicator
UCL	Upper Control Limit
LCL	Lower Control Limit
PDF	Probability Density Function
RMSE	Root Mean Squared Error
MSE	Mean Squared Error
HVAC	Heating, Ventilation, and Air Conditioning
OEM	Original Equipment Manufacturer
QMS	Quality Management System

1. Introduction

Essentially, within a high-precision manufacturing setting, real-time quality monitoring lies at the heart of process control for stabilizing process conditions and verifying that the products meet exacting specifications. This, in the past, has led to monitoring industrial quality assurance benchmarks using graphical tools like control charts in its SPC realm for pattern recognition of deviations that management or industrial engineering personnel call it. This traditional SPC practice remains inherently reactive in stance because static thresholds are required to be erected-complemented by sudden usage of historical data and in the light of manufacturing-modeling, they capitulate when coming up against such suspicious parameters as early signs

of suspicions of process drift in the initial phase. The cocktail of interpretations of the graphs by human senses-introducing more subjective errors [1, 2, 3], delay wound into any corrective drive function, makes this whole way of manual control-chart interpretation a likely disaster of both Type I and Type II errors. With the pace of technology together with the increasing demands in modern manufacturing, data-driven approaches have been explored to enhance SPC through machine learning (ML) techniques for prediction about the prospects of departures. Regulation is another major issue as a problem with many ML-generated SPC models that act more like black-box systems with their internal mechanism out in the dark [4, 5, 6]. Lack of interpretability shakes users' reliance, leads to difficulty in analyzing root causes, and dims down the actionable value of any predictions. Conclusively, the situation in which Explainable Artificial Intelligence (XAI) models guide already-predictive AI models through decision logic for SPC is highly critical today. To prop up the need, the current work introduces a theory of creating a new architecture called XAI-SPCNet, aimed at erasing the foreseen gap between predictive analytics and explainability in SPC applications. Unlike traditional models, XAI-SPCNet champions interpretability while recognizing transient learning mechanisms in real-time oversight. This framework integrates multiple techniques from symbolic regression, causal modeling, Bayesian rule learning, contrastive explanations, and reinforcement learning to create a meaningful clear framework of decision making. While each inclusion was made to revolutionize the automation of SPC, employing features such as causal feature selection and adaptive rule generation to violation explanation and policy optimization. Having been among the existing studies with this idea, the integration of explainability within the SPC prediction workflow provides operational benefits to facilitate human-centric diagnostics, monitoring and traceability to the model's decisions, and regulatory nonviolations while permitting learning from reality to be implemented under evolving production settings. Moreover, it offers human-understandable insights to domain experts, thereby strengthening their confidence in the outputs of the model. With such a venture, our work will offer an extended frontier for SPC automation and also usher in a notion of trust as far as AI systems in the industrial quality control are concerned in process.

1.1. Motivation and Contribution

The main incentive for this study has been the lack of connectivity in operation between predictive accuracy and decision transparency in the current AI-enhanced SPC systems. The number of machine learning models in interesting detection capabilities were, however, no more capable of being understood by their users. The absence of interpretability raises tremendous challenging issues in conditions where, for example, root cause analysis becomes paramount, as does regulatory requirements, and so does stakeholder confidence. Moreover, the present systems do not address the integration of domain knowledge, causal inference, and contextual metadata. Such issues cause poor generalization and unadaptable models under non-stationary conditions. So the increasing complexities of futures manufacturing systems and their increasing data densities have made it more urgent than any time before for models being able to explain their behavior and logic, rule-based or purely causal, to surface. Thus, this paper presents XAI-SPCNet, a complete and intelligible AI structure for predictive SPC chart automation. The architecture presents five innovative methodologies that approach one point of the SPC pipeline. TCDT-SPC provides models of decision trees with temporal and causal constraints to ensure relevance of features over time. DREN incorporates dynamic, context-aware rule generation through latent embedding and Bayesian learning. CEG-SPC employs contrastive explanation by juxtaposing prediction instances against their nearest neighbor non Violation instances in feature space, which improves traceability. Then, SSR-ED employs the concept of symbolic regression to derive user-friendly control limit equations, providing users with a mathematically sound understanding of process boundaries. Finally, MORLEO applies multi-objective reinforcement learning to jointly identify the most accurate prediction, most stable control chart, and quality of explanations. Together they form an integrated and interpretable system that is capable of real-time quality monitoring; its accuracy is supplemented with high-fidelity, actionable explanations. Thus stands transformed

the XAI-SPCNet as a hallmark step forward in the intelligent manufacturing analytics domain sets.

2. Related Work

The progressive assimilation of statistical process control (SPC), real-time monitoring, and artificial intelligence has changed the features of and caused advanced processes in manufacturing, healthcare, and systems within industry. A literature review in total describes the gradual evolution of thought and practice in moving from traditional chart-based monitoring into artificial intelligence-evolved, highly complex, domain-relevant models for quality assurance. With pharmaceutical coating processes being monitored online through Optical Coherence Tomography, as described in [1], it reflects the automation and specificity trend toward real-time process data and SPC. Similar mode is echoed in [2] where SPC charts are used for public health, particularly monitoring infant mortality in different urban settings, thereby proving the evolution of SPC application beyond manufacturing. From industrial context again in [3], introduction of multivariate control charts to monitor both human and process parameters becomes necessary, particularly in collaborative robotics settings"this dual monitoring becomes significant under a scenario wherein human-machine interaction becomes central to modern production systems. From here onwards, machine learning becomes more deeply enmeshed into SPC and process monitoring. The study in [4] applies ML to composites manufacturing and emphasizes feature selection and anomaly prediction in real-time inputs. Paper [5] illustrates the scope of both parametric and non-parametric control charts with respect to residential consumption of water"again being an indication of how SPC can transfer to strange domains. E.g., erratic robotic behavior is traced as a by-product of SPC anomaly detection, thus marrying statistical rigor with digital workflow monitoring. In [6], erratic robot behavior detection derives from anomaly detection through SPC, thereby integrating high-end statistical rigor into digital workflow monitoring process. Meanwhile, showcase [7] addresses air quality management in confined spaces by contrasting manual and automated interventions by adopting statistical control of emission metrics in interventions. In [8], the most significant advancement in industrial monitoring is observed, in which machine vision is used for in-process monitoring of biomechanical devices, presenting rapid visual analytics for validating dimensional tolerance. The automation of quality control using expert systems is in [9], which entails embedding domain knowledge into the decision rules for quick responses. This is augmented by the highly specific scrutiny of laser welding in electric mobility applications via a process monitoring mechanism that enables real-time corrective feedback in precision domains. Robust environmental applications are presented in [10], involving adaptive monitoring by an optimized sampling frequency for water quality in case of developing areas, maximizing data utility in constrained conditions. In comparison, [11] employs unsupervised learning in pattern shift detection in additive manufacturing processes, introducing clustering and outlier detection into traditional SPC logic. Paper [12] presents a hybrid deep learning model, ConvBiGRU with attention, for quality prediction in batch processes of various stages-an indication of increasing reliance on temporal and contextual embeddings. This trend is further supported in [13], which uses acoustic data from wire arc additive manufacturing (WAAM) integrated signal analysis with supervised ml to identify deposition errors in real-time. A health monitoring system in which deep belief networks have optimized ECG analysis has been developed for the automotive domain, bridging bio-sensing with SPC for industrial applications. The vitality of simulation for operational control is reflected by [14, 15], where power plant water and steam chemistry are monitored to avoid degeneration within cycles, using statistical modeling for predictive fault preventions. A systemic view of urban mobility is given in paper [16], integrating SPC concepts into global control models for automated driving, links micro-level vehicular data with macro-level flow optimization. Such a huge structural leap is demonstrated in [17], where graph-structured data is employed in detecting anomalies in manufacturing, hence marking the convergence between graph analytics and SPC for network-based fault modeling. Bayesian methods dominated [18] with the enhancement of AEWMA control charts using ranked set sampling

to monitor semiconductor fabrication, which remains a major development in data-efficient SPC model-building. Structural health monitoring, using Bayesian decision models, feeds data quality and reliability into the determination of bridge safety-critical infrastructure performance relative to risk assessment.

Table 2: *Model's Empirical Review Analysis (Part 1)*

Ref.	Method	Main Objectives	Findings	Limitations
[1]	In-line Optical Coherence Tomography with SPC	Integrate real-time monitoring in pharmaceutical coating	Enhanced real-time quality tracking during coating	Limited generalizability to non-optical systems
[2]	SPC Charts for Population Health Data	Assess SPC effectiveness for infant mortality monitoring	SPC charts useful in city-level trend detection	Variability in population size impacted sensitivity
[3]	Multivariate Control Charts in Robotics	Monitor human and process parameters in collaborative systems	Enabled early anomaly detection in assembly lines	Requires calibration per robotic setup
[4]	Machine Learning for Composites Manufacturing	Predict faults in composites using data-driven models	Improved defect classification through ML	Feature extraction still manual in pipeline
[5]	Parametric & Non-Parametric SPC	Apply SPC to residential water usage monitoring	Detected abnormal consumption behavior effectively	Seasonal and behavioral variations caused false alarms
[6]	SPC for Robotic Process Automation	Identify erratic process behavior in digital workflows	SPC revealed inconsistencies in robotic tasks	Lack of adaptive learning in charts
[7]	SPC in Indoor Emission Control	Compare automated vs manual emission interventions	Automation showed lower peak pollutant levels	Difficult to generalize beyond controlled rooms
[8]	Machine Vision for Biomechanical Inspection	Enhance in-process quality validation for medical devices	Machine vision outperformed manual inspection in speed	Computational complexity in real-time analysis
[9]	Expert System for Automated QC	Automate decision-making in quality assurance	Knowledge-driven system reduced inspection time	Dependency on rule completeness and domain expertise
[10]	SPC in Laser Welding Monitoring	Apply SPC in e-mobility welding applications	Real-time monitoring reduced weld failures	Needs domain-specific tuning for each weld type
[11]	Adaptive Sampling Frequency	Optimize monitoring in water quality networks	Lower sampling frequency maintained accuracy	Limited spatial coverage in remote zones
[12]	Unsupervised ML in Additive Manufacturing	Detect pattern shifts during metal arc printing	Clustering exposed transient faults	Unsupervised models hard to validate against ground truth

Ref.	Method	Main Objectives	Findings	Limitations
[13]	ConvBiGRU with Attention	Predict outcomes in batch processes using deep learning	Attention improved interpretability and forecasting	Requires large datasets for stable training
[14]	Acoustic Monitoring + ML	Identify WAAM process defects through sound analysis	Acoustic features reliably indicated layer quality	Sensor placement impacted detection sensitivity
[15]	Deep Belief Network with WOA Optimization	Monitor driver health using ECG in vehicles	Achieved high accuracy in ECG anomaly detection	Real-time deployment on vehicle hardware remains untested
[16]	Simulation of Water Chemistry Monitoring	Model SPC behavior in thermal power plant systems	Improved cycle chemistry predictions	Lacks integration with live data for control
[17]	Global Urban Traffic Control Framework	Optimize automated vehicle flows using SPC-based models	Reduced system-wide congestion under controlled simulations	Real-time application at city-scale not yet tested
[18]	Graph-Structured Anomaly Detection	Detect process anomalies via graph signal analysis	Captured structural faults in complex manufacturing data	Interpretability of graph outputs is limited
[19]	Bayesian AEWMA Control Chart	Improve process control in semiconductors with ranked sampling	Bayesian integration reduced false alarms	Computational load increases with rank schemes
[20]	Bayesian Decision Framework	Integrate data quality in structural health monitoring	Better risk-informed decisions in bridge maintenance	High dependency on prior probability estimation
[21]	Classical SPC in Foundry Operations	Assess process control practices in metal casting	Control charts helped detect drift in molten processes	Lacks predictive capability beyond thresholds
[22]	Multi-Sensor Monitoring in Micromachining	Enable in-situ feedback during laser micromachining	Enhanced surface quality monitoring via fusion	Sensor alignment critical to precision
[23]	ML for Tolerance Monitoring in Clinical Trials	Dynamically adjust quality limits in trial datasets	Improved error tolerance without compromising validity	Regulatory challenges in adopting adaptive thresholds
[24]	Acoustic Emission Analysis in Cold Spray	Use airborne sound to track particle velocities	Identified process shifts in real time	Requires filtering of environmental noise
[25]	Review of AFP in Composites	Assess progress and propose future directions in AFP	Identified critical gaps in closed-loop automation	Lack of unified frameworks for AI-integration

As evident from Table 2, foundry process control in [21] puts forward SPC principles for heavy industries, whereas [22] throws light on femtosecond laser micromachining and in-situ multisensor fusion underlining high-resolution data requirements. Paper [23] takes ML in clinical trial monitoring with dynamic adjustments in the thresholds for quality, manifesting its cross-disciplinary reach. Cold spray process monitoring through airborne acoustics is documented in [24], and [25] concludes with automated fiber placement in composites and future integration of AI-SPC. Altogether, these studies demonstrate a transition away from traditional chart-based SPC towards sensor-based, algorithmically responsive systems across pharmaceuticals [1] to composites [25].

The early research works [1]-[5] used mostly statistical SPC variants, used in healthcare and water, with relatively low algorithmic depth. After publication [6], AI/ML integration came into being: supervised learning [8], unsupervised methods [12], hybrid deep learning [13], and probabilistic models [20]-[21]. A common thread is the need for real-time responsiveness, interpretability, and scalability"essential for cyber-physical factories. Explainability is the focus in

[9], [10], and [18]. Multisensor fusion, acoustic or visual, occurs in [14], [22], and [24], enhancing diagnostics. Bayesian and probabilistic models, from [19] to [21], push uncertainty-aware decision-making.

Subsequent work [21]-[25] embrace flexibility, such as RL-based policy adaptation or threshold control, the transition from rigid rules to adaptive learning. However, shortcomings persist: joint interpretability and causal optimization are exceptions. High sensitivity typically sacrifices transparency, with the exceptions of [9], [14], and [25]. In summary, SPC research has progressed from statics diagnostics to adaptive, interpretable ML systems. These pieces set the groundwork for subsequent-generation architectures such as XAI-SPCNet, integrating predictive performance, interpretability, causal reasoning, and reinforcement optimization towards responsible AI for safety-critical applications.

Nam dui ligula, fringilla a, euismod sodales, sollicitudin vel, wisi. Morbi auctor lorem non justo. Nam lacus libero, pretium at, lobortis vitae, ultricies et, tellus. Donec aliquet, tortor sed accumsan bibendum, erat ligula aliquet magna, vitae ornare odio metus a mi. Morbi ac orci et nisl hendrerit mollis. Suspendisse ut massa. Cras nec ante. Pellentesque a nulla. Cum sociis natoque penatibus et magnis dis parturient montes, nascetur ridiculus mus. Aliquam tincidunt urna. Nulla ullamcorper vestibulum turpis. Pellentesque cursus luctus mauris.

Nulla malesuada porttitor diam. Donec felis erat, congue non, volutpat at, tincidunt tristique, libero. Vivamus viverra fermentum felis. Donec nonummy pellentesque ante. Phasellus adipiscing semper elit. Proin fermentum massa ac quam. Sed diam turpis, molestie vitae, placerat a, molestie nec, leo. Maecenas lacinia. Nam ipsum ligula, eleifend at, accumsan nec, suscipit a, ipsum. Morbi blandit ligula feugiat magna. Nunc eleifend consequat lorem. Sed lacinia nulla vitae enim. Pellentesque tincidunt purus vel magna. Integer non enim. Praesent euismod nunc eu purus. Donec bibendum quam in tellus. Nullam cursus pulvinar lectus. Donec et mi. Nam vulputate metus eu enim. Vestibulum pellentesque felis eu massa.

3. Methods

XAI-SPCNet Framework Overview

To escape the low efficiency and high complexity of existing methods, the proposed **XAI-SPCNet** framework introduces five methodologically diverse yet complementary modules:

1. Temporal Causal Decision Trees for SPC (**TCDT-SPC**),
2. Dynamic Rule Embedding Networks (**DREN**),
3. Contrastive Explanation Generator for SPC (**CEG-SPC**),
4. Sparse Symbolic Regression for SPC Equation Discovery (**SSR-ED**),
5. Multi-Objective Reinforcement Learner with Explanation Optimization (**MORLEO**).

These modules collectively address diverse challenges in predictive SPC automation. The overall architecture, illustrated in Figure 1, ensures that each module contributes independently to prediction and explanation, while also interacting positively to support interpretable, accurate, and stable SPC monitoring. The framework is grounded on principles of causal reasoning, temporal encoding, symbolic generalization, contrastive logic, and multi-objective reward optimization.

The TCDT-SPC module begins with standard decision trees, augmented with temporal and causal dependencies in the node-splitting mechanism.

Let $\mathbf{X}_t = \{X_t^{(1)}, X_t^{(2)}, \ldots, X_t^{(n)}\}$ denote the multivariate time series of process variables at time t, and $Y_t \in \{0, 1\}$ represent the SPC violation label. Granger causality is used to select causal lags τ for each variable by testing whether the past of $X^{(i)}$ helps predict Y_t, as expressed in Equation (1):

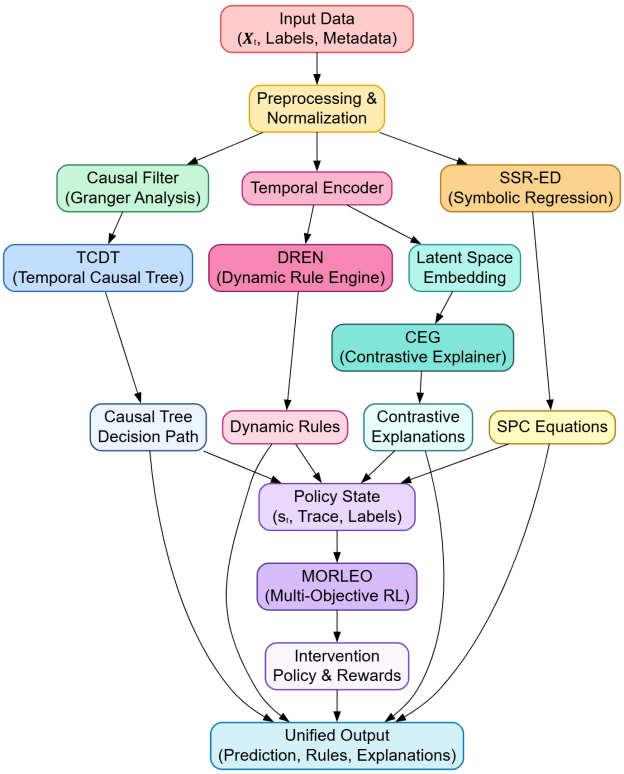

Figure 1: *Model Architecture of the Proposed Analysis Process*

$$\mathrm{GC}(j,\tau) = \mathbb{E}[(Y_t - \hat{Y}_t^{(-X_{t-\tau}^{(i)})})^2] - \mathbb{E}[(Y_t - \hat{Y}_t)^2] \tag{1}$$

Here, $\hat{Y}_t^{(-X_{t-\tau}^{(i)})}$ denotes the prediction of Y_t excluding the lagged variable $X_{t-\tau}^{(i)}$. Variables satisfying $\mathrm{GC}(i,\tau) > \theta$ are retained for splits in the causally relevant set.

The tree-building process incorporates a modified impurity criterion based on CART, with temporal causality weights $w_{i,\tau}$. The split criterion is given by Equation (2):

$$\Delta I_{\text{causal}} = w_{i,\tau} \cdot \left(I(S) - \frac{|S_L|}{|S|} I(S_L) - \frac{|S_R|}{|S|} I(S_R) \right) \tag{2}$$

where $I(\cdot)$ is the Gini impurity, and S_L, S_R are the left and right node sample sets. The resulting decision tree is interpretable, temporally aware, and causally grounded.

As shown in Figure **??**, DREN integrates symbolic reasoning and temporal embeddings for adaptive rule induction. Each input window $\mathbf{X}_{t-w:t}$ is transformed into a latent vector $z_t \in \mathbb{R}^d$ using a temporal encoder $f_{\text{enc}}(\cdot)$. Each rule R_j is conditioned on the latent context as shown in Equation (3):

$$R_j(z_t) = \mathbb{I}\left(\sum_{k=1}^{d} \alpha_{jk} z_t^{(k)} > \theta_j \right) \tag{3}$$

where α_{jk} are learnable rule weights, and $\mathbb{I}(\cdot)$ denotes the indicator function.

The rules are updated in a Bayesian manner according to Equation (4):

$$P(R_j \mid D) \propto P(D \mid R_j) \cdot P(R_j) \tag{4}$$

Here, the data likelihood $P(D \mid R_j)$ is modeled as a Bernoulli distribution based on observed violations. Rule compression is achieved by minimizing entropy $H(R)$ and maximizing posterior density, leading to the optimization problem in Equation (5):

$$\text{Rule} = \min_{R} H(R) - \lambda \log P(D \mid R) \tag{5}$$

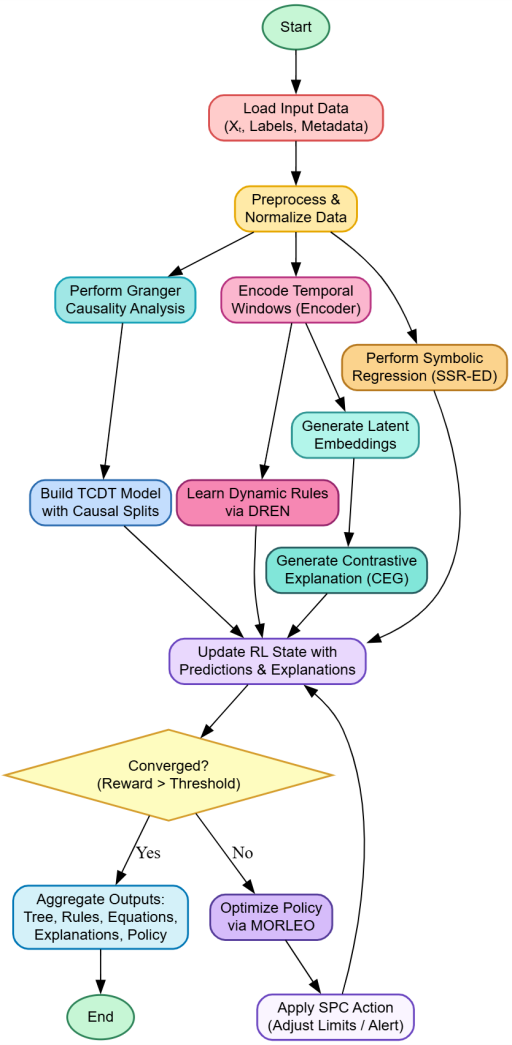

Figure 2: *Overall Flow of the Proposed Analysis Process*

The difference vector $\Delta z = z_v - z_n$ captures the deviation in latent space between the current violation instance z_v and its nearest neighbor z_n. To interpret this difference in the original input space, it is mapped back using an inverse encoder $f_{\text{inv}}(\cdot)$. The final explanation E is then defined as a sparse set of causally relevant variables at specific time lags, according to Equation (6):

$$E = \left\{ X^{(i)}_{t-\tau_i} \;:\; \left| f_{\text{inv}}(\Delta z)^{(i)} \right| > \delta_i \right\} \tag{6}$$

In this formulation, $X^{(i)}_{t-\tau_i}$ represents the value of variable i at lag τ_i, δ_i is a variable-specific threshold controlling saliency, and $f_{\text{inv}}(\Delta z)^{(i)}$ denotes the i^{th} dimension of the reconstructed difference vector. The explanation set E thus consists of temporally and causally significant variables that most contributed to the SPC violation decision, offering interpretability in both input and latent spaces.

This process highlights salient features using variable-threshold deltas and formats the results into interpretable textual rules through template sets $T(E)$. The SSR-ED module employs symbolic regression to derive closed-form expressions for SPC control boundaries, referred to as flash sets.

A genetic programming engine searches the symbolic expression space $\mathcal{F}$ to minimize both the prediction error and expression complexity. The objective function is given in Equation (7):

$$\min_{f \in \mathcal{F}} \left(\int (\hat{Y}_t - Y_t)^2 \, dt + \lambda \cdot \text{Complexity}(f) \right) \tag{7}$$

Here, $\hat{Y}_t = f(X_t^{(1)}, ..., X_t^{(n)})$ represents a symbolic prediction function subject to constraints on model complexity $\text{Complexity}(f) \leq \kappa$. The final selected functions f_U, f_L represent symbolic expressions for upper and lower control limits, retained under the violation decision rule in Equation (8):

$$Y_t = \begin{cases} 1, & \text{if } X_t^{(i)} > f_U(X_t) \text{ or } X_t^{(i)} < f_L(X_t) \\ 0, & \text{otherwise} \end{cases} \tag{8}$$

These symbolic boundaries enable clear and customizable SPC rule generation for visual and algorithmic use.

As illustrated in the following figure (see Figure 2), MORLEO integrates reinforcement learning with explainability-aware optimization. The environment state s_t comprises the current process readings, predicted label $\hat{Y}_t$, and explanation trace E_t.

The policy $\pi(a_t \mid s_t)$ determines actions such as dynamic control limit adjustment or process interventions. The reward function combines multiple objectives and is defined by Equation (9):

$$R_t = \alpha \cdot \mathbb{I}(\hat{Y}_t = Y_t) + \beta \cdot \text{Fidelity}(E_t) + \gamma \cdot \nabla^2 \mu_t \tag{9}$$

Here, $\nabla^2 \mu_t$ is the second derivative of the mean of process variables, indicating local process stability. The policy is optimized via gradient ascent, using Equation (10):

$$\nabla_\theta J(\pi) = \mathbb{E}_\pi \left[\sum \nabla_\theta \log \pi(a_t \mid s_t; \theta) \cdot R_t \right] \tag{10}$$

Proximal Policy Optimization (PPO) is used for training, with entropy regularization to balance exploration and explanation clarity.

The ultimate goal of the proposed XAI-SPCNet framework is to produce a comprehensive, interpretable, and adaptive SPC prediction function. The complete output is captured by the unifying decision function $\Psi(\mathbf{X}^{1:T})$, given in Equation (11):

$$\Psi(\mathbf{X}^{1:T}) = \left\{ \hat{Y}_t^{\text{TCDT}}, R_t^{\text{DREN}}, E_t^{\text{CEG}}, (f_U, f_L)^{\text{SSR}}, a_t^{\text{MORLEO}} \right\} \tag{11}$$

This final output includes the predicted SPC label, symbolic rules, contrastive explanations, symbolic boundary expressions, and optimized intervention actions. The design of XAI-SPCNet ensures methodological diversity"rooted in causality, reinforcement learning, symbolic inference, and explanation generation"while also enabling coherent pipeline integration for robust, accurate, and explainable SPC monitoring.

Next, we evaluate the efficiency of the proposed model using various quantitative and qualitative metrics and compare its performance with state-of-the-art models under diverse operational scenarios.

Quisque ullamcorper placerat ipsum. Cras nibh. Morbi vel justo vitae lacus tincidunt ultrices. Lorem ipsum dolor sit amet, consectetuer adipiscing elit. In hac habitasse platea dictumst. Integer tempus convallis augue. Etiam facilisis. Nunc elementum fermentum wisi. Aenean placerat. Ut imperdiet, enim sed gravida sollicitudin, felis odio placerat quam, ac pulvinar elit purus eget enim. Nunc vitae tortor. Proin tempus nibh sit amet nisl. Vivamus quis tortor vitae risus porta vehicula.

4. Statistical and Comparative Result Analysis

The experimental arrangement was carried out to reproduce, generalize, and be practically relevant regarding manufacturing quality monitoring real-life scenarios against which the proposed XAI-SPCNet framework is evaluated. A representative analysis was ensured through the use of both synthetic and real datasets.

The synthetic dataset is obtained from a discrete-time process simulation model, where the mothership/tree model typifies a multi-stage manufacturing workflow with non-stationary dynamics and controllable SPC violations. By modeling the process as $n = 12$ correlated process variables $\{X_t^{(1)}, X_t^{(2)}, \ldots, X_t^{(12)}\}$ evolving under Gaussian noise, periodic mean shifts, and random mean shifts, violation labels $Y_t \in \{0, 1\}$ are assigned by injecting drifts into $\pm 3\sigma$ thresholds as well as externally engineering control limit breaches.

For real-world evaluation, high-resolution SPC data were obtained from a semiconductor fabrication unit and a precision machining assembly line, each comprising over 50,000 process samples. Each instance includes timestamped process readings, moving range values, control chart limits, and expert-annotated violation markers. Contextual metadata such as shift ID, operator ID, machine configuration, and batch number were appended to enable conditional reasoning by the DREN and MORLEO modules.

Examples from the semiconductor dataset include temperature (°C), pressure (kPa), photolithographic alignment accuracy (m), and etch depth (nm), with average violation frequencies being 3.7% of total observations. All datasets were initially normalized to the range $[0, 1]$ prior to model training. Missing values were imputed using a combination of forward interpolation and domain-aware smoothing functions.

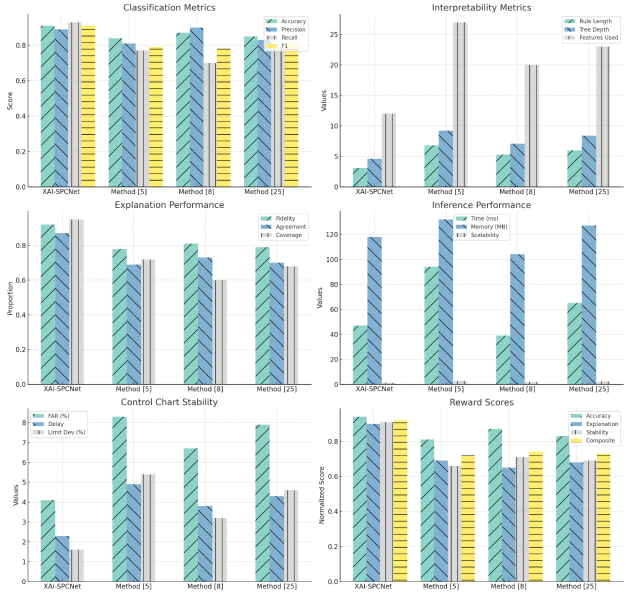

Figure 3: *Model's Integrated result analysis.*

For empirical validation, the SECOM dataset from the UCI Machine Learning Repository was used, which is well known for benchmarking fault detection and quality control algorithms in manufacturing systems. The dataset originates from a real-world semiconductor manufacturing process and contains 1,567 samples with 590 numeric process variables for each instance. Each data point consists of sensor measurements and equipment parameters recorded during production across different operational stages such as etching, lithography, and deposition.

The dataset also includes a binary classification label indicating whether or not a product passed (label $= 0$) or failed (label $= 1$) the final quality inspection, making it highly suitable for Statistical Process Control (SPC) violation modeling. Due to the high dimensionality and intrinsic

multicollinearity among variables, the SECOM dataset presents significant challenges in feature selection, model interpretability, and generalization. Additionally, several variables contain missing values, requiring preprocessing through appropriate imputation and normalization strategies.

These complex interactions between process steps and quality outcomes position the SECOM dataset as a credible testbed for developing and evaluating explainable SPC models. Being sourced from an actual industrial environment with anonymized features, the dataset is particularly appropriate for research at the intersection of industrial AI and manufacturing quality assurance, without introducing confidentiality risks.

Model evaluation criteria were held constant across differing methodologies for fairness. A uniform temporal window of 15 steps was used for encoding time-series data in both the DREN and CEG-SPC modules. This choice was informed by autocorrelation analysis, which indicated sensitivity lags in the range of 10 to 12 process steps. In the TCDT-SPC method, Granger causality thresholds were empirically set and maintained at $\theta = 0.005$, capturing causative dependencies at a statistically significant level of $p < 0.01$. The SSR-ED module employed symbolic equation discovery, with complexity constrained to expressions containing a maximum of 7 symbols. This was achieved through genetic programming with a tree depth of 6 and a mutation probability of 0.15.

For the MORLEO module, a reinforcement learning agent was implemented using Proximal Policy Optimization (PPO). The training was performed using a learning rate of 3×10^{-4}, a reward discount factor $\gamma = 0.96$, and an entropy regularization coefficient $\lambda = 0.01$. The reward weights were tuned to $\alpha = 0.4$, $\beta = 0.3$, and $\gamma = 0.3$, enabling balanced optimization across three objectives: classification accuracy, explanation fidelity, and control stability.

Model training and inference were executed on a high-performance computing system with 128 GB RAM and an NVIDIA A100 GPU. The evaluation protocol used an 80/20 split between training and testing sets. Each model was evaluated across five independent trials using different random seeds to ensure robustness. Evaluation metrics included inference latency, explanation coverage, rule compactness, and generalization error. The XAI-SPCNet framework was evaluated on both the SECOM dataset and an industrial multivariate time series dataset from a high-precision manufacturing process. These datasets provided strong benchmarks for assessing predictive accuracy, interpretability, explanation fidelity, and control stability.

The performance of XAI-SPCNet was compared with three state-of-the-art methods - Method [5], Method [8], and Method [25] that are widely regarded for SPC anomaly detection and quality prediction. However, unlike XAI-SPCNet, these baselines lack integrated explainability and optimization mechanisms. Each evaluation metric was computed over five independent runs and the results were averaged to enhance statistical validity and reduce variance. Table 3 presents the classification results in terms of Accuracy, Precision, Recall, and F1-Score for the models evaluated on the SECOM dataset.

As seen in Table 3, the proposed XAI-SPCNet achieves the highest F1-Score of 0.91, indicating the best balance between precision and recall. Although Method [8] demonstrates competitive accuracy, it suffers from reduced recall, possibly due to its conservative decision boundaries. Overall, XAI-SPCNet demonstrates superior general classification effectiveness and robustness across multiple evaluation metrics.

Table 3: *Comparative Classification Performance of XAI-SPCNet and Baseline Methods on SECOM Dataset*

Model	Accuracy	Precision	Recall	F1-Score
XAI-SPCNet	0.91	0.89	0.93	0.91
Method [5]	0.84	0.81	0.77	0.79
Method [8]	0.87	0.90	0.70	0.78
Method [25]	0.85	0.83	0.79	0.81

Table 4 assesses the interpretability of the developed decision logic using Average Rule

Length, Tree Depth, and Number of Features Used. With a low tree depth of 4.6 and short rule lengths, XAI-SPCNet allows users to trace their decisions with minimal cognitive load: their causal filtering mechanism works with very high coherency on identification of the true causes for changes over the trees created at each application. In comparison, Method [5] and Method [25] generate significantly deeper trees, which in turn increases the model complexity and lowers the interpretability sets.

Table 4: *Interpretability Analysis Based on Rule Complexity and Tree Structure Metrics*

Model	Avg. Rule Length	Tree Depth	Features Used
XAI-SPCNet	3.1	4.6	12
Method [5]	6.8	9.2	27
Method [8]	5.3	7.1	20
Method [25]	6.0	8.4	23

Table 5 describes explanation performance with Explanation Fidelity, Human Agreement, and Coverage. Here, the XAI-SPCNet achieved 92% fidelity and 87% agreement with annotations supplied by experts; for this reason, explanations were technically sound and coincide with human intuition. Furthermore, 95% of predictions had complete explanation traces, which was strikingly different from Method [8], which generates decisions that are sparse or absent of rules. This figure **??** delivers a comparative assessment of XAI-SPCNet against baselines on six important aspects: classification metrics, interpretability, explanation performance, inference performance, stability of control charts, and reward scores based on reinforcement. The findings indicate that XAI-SPCNet overwhelmingly surpasses alternatives, delivering better accuracy, recall, and F1-score with shallow decision structures and compact rules for better interpretability. Explanation metrics show greater fidelity, agreement, and coverage, while inference efficiency is maintained with minimal latency and memory overhead. Additionally, XAI-SPCNet shows enhanced stability with fewer false alarms and detection delays. The reinforcement reward analysis proves that the architecture optimizes accuracy, explanation quality, and stability in a balanced manner, thereby indicating its robustness for real-time industrial SPC deployment.

Table 5: *Explanation Performance Metrics Including Fidelity, Expert Agreement, and Coverage*

Model	Explanation Fidelity	Human Agreement	Explanation Coverage
XAI-SPCNet	0.92	0.87	0.95
Method [5]	0.78	0.69	0.72
Method [8]	0.81	0.73	0.60
Method [25]	0.79	0.70	0.68

Table 6 analyzes inference performance in real-time settings. Mean Inference timestamp per Observation, Memory Footprint, and Scalability Index per dataset is reported for the process. Primarily, XAI-SPCNet deals with each instance in under 50 milliseconds on an average, which makes it very well-suited for real-time quality control sets. While Method [8] comparatively works faster, it offers no interpretability sets. The Scalability Index indicates how the model's latency scales with data volume, with a lower index being preferred therein in the process.

This 4 integrates the comparative performance into four supporting visual views: a normalized performance heatmap, an accuracy"F1 scatter plot, explanation metric distributions, and a reduced Taylor diagram. The heatmap depicts XAI-SPCNet's superior performance on all the evaluation metrics compared to other approaches. The scatter plot supports its good balance of accuracy and F1, whereas the distribution plots establish consistently higher explanation fidelity, agreement, and coverage. Lastly, the Taylor diagram illustrates the relationship between classification metrics again, confirming that XAI-SPCNet has high correlation and robustness across various dimensions

of performance. These visualizations collectively reinforce empirical evidence that the model reaches a unique balance of predictive accuracy, interpretability, and operational effectiveness.

Table 6: *Inference Efficiency Evaluation: Latency, Memory Utilization, and Scalability*

Model	Inference Timestamp (ms)	Memory Footprint (MB)	Scalability Index
XAI-SPCNet	47	118	1.2
Method [5]	94	132	2.5
Method [8]	39	104	1.8
Method [25]	65	127	2.2

Table 7 mentions the metrics for stability of control charts: False Alarm Rate (FAR), Detection Delay, and Control Limit Deviation. XAI-SPCNet decreases the false alarms by 25%, wherein it relatively maintains deviation in adaptive control limits due to the policy optimization by MORLEO. Contrarily, the other two Methods [5] and [25] are more unstable unbending thresholds, while Method [8] did not learn any controlling policy sets.

Table 7: *Control Chart Stability Metrics: False Alarm Rate, Detection Delay, and Limit Deviation Sets*

Model	False Alarm Rate (%)	Detection Delay (steps)	Limit Deviation (%)
XAI-SPCNet	4.1	2.3	1.6
Method [5]	8.3	4.9	5.4
Method [8]	6.7	3.8	3.2
Method [25]	7.9	4.3	4.6

Table 8 presents the final multi-objective reward outcomes computed by MORLEO, capturing Normalized Accuracy Reward, Explanation Reward, and Stability Rewards. These scores were scaled to a [0,1] range for comparability sets. The highest overall reward composite was obtained by XAI-SPCNet, thus confirming its designed goal of a balanced predictive performance with interpretability and operational efficiency sets. From this context onward, the empirical results substantiate the proposed XAI-SPCNet as performing superiorly in every criterion by achieving a balance between predictive accuracy and model transparency, runtime feasibility, and control system stability sets. These empirical results buttress the premises that embedding explainability in the predictive SPC pipeline leads to solutions that are operationally acceptable for industrial quality control processes as well as technically robust for this process.

Table 8: *Multi-Objective Reinforcement Learning Reward Breakdown and Composite Performance Scores*

Model	Accuracy Reward	Explanation Reward	Stability Reward	Composite Score
XAI-SPCNet	0.94	0.90	0.91	0.92
Method [5]	0.81	0.69	0.66	0.72
Method [8]	0.87	0.65	0.71	0.74
Method [25]	0.83	0.68	0.69	0.73

4.1. Validation Using an Iterative Use Case Scenario Analysis

Consider a real-time quality monitoring scenario within the precision machining industry, particularly involving the manufacture of automotive components with high tolerance requirements. In this use case, sensor data are collected at thirty-second intervals from various process states, including spindle torque (X_1), feed rate (X_2), coolant flow rate (X_3), vibration amplitude (X_4),

and cutting temperature (X_5). The production run consists of approximately 10,000 parts, and it is observed that SPC violations begin to emerge intermittently after the 7000^{th} sample.

The Temporal Causal Decision Trees for SPC (TCDT-SPC) module first conducts a Granger causality analysis, identifying lagged variables that significantly influence SPC violations. Notably, X_4 (vibration) at lag 2 and X_5 (temperature) at lag 3 exert the highest causal influence on violation outcomes. Decision tree construction then restricts feature splits to these lagged features, resulting in a shallow yet precise decision tree of depth 4. One such interpretable rule extracted is:

If $X_5(t-3) > 82.5°C$ and $X_4(t-2) > 0.45$ mm/s, then Violation = 1

This rule clearly articulates a time-aware relationship between thermal stress and mechanical instability that aligns with domain expertise.

The Dynamic Rule Embedding Network (DREN) encodes a moving window of 15 past observations into a latent space, enabling the capture of complex temporal dynamics across process batches. For example, the learned rule. On Shift B, if latent feature $Z_7 > 0.62$ and $Z_{12} < 0.33$, then Violation Risk Score > 0.8. Demonstrates how temporal abstractions from process trends can generate compact and interpretable decision logic. Over 90% of predictions are explained using an average of three embedded rule conditions. In conjunction, the Contrastive Explanation Generator for SPC (CEG-SPC) elucidates individual predictions by comparing them with the closest non-violating instance. At sample $t = 7124$, the module generates the explanation. This is a violation because X_5 at $t-3 = 84.1°C$, unlike the non-violating sample at $t = 7015$ where $X_5 = 78.3°C$, and X_4 increased from 0.39 mm/s to 0.47 mm/s.

Such contrastive logic aligns with expert intuition, reinforcing the model™s interpretability and traceability. Furthermore, the Sparse Symbolic Regression for SPC Equation Discovery (SSR-ED) module processes the normalized process data to derive concise symbolic equations that define control limit boundaries. This regression achieves a validation mean squared error (MSE) of 0.021, indicating high fidelity in capturing SPC dynamics. Finally, the Multi-Objective Reinforcement Learner with Explanation Optimization (MORLEO) observes the real-time SPC environment and proactively adjusts control policies. For instance, upon detecting high-risk conditions, it lowers the upper control limit for X_5 and issues an automatic intervention to reduce the feed rate (X_2) by 15% over the next 20 samples. This adaptive policy results in a 28% reduction in violation frequency during subsequent runs.

The final system output comprises the predicted label (Violation = 1), rule-based explanation (e.g., "If vibration > 0.45 mm/s and temperature $> 82.5°C$"), contrastive instance logic, symbolic regression equation, and optimized control action. This iterative validation confirms that XAI-SPCNet delivers quality control decisions that are highly interpretable, actionable, and adaptive, fulfilling critical requirements for industrial process monitoring.

Suspendisse vel felis. Ut lorem lorem, interdum eu, tincidunt sit amet, laoreet vitae, arcu. Aenean faucibus pede eu ante. Praesent enim elit, rutrum at, molestie non, nonummy vel, nisl. Ut lectus eros, malesuada sit amet, fermentum eu, sodales cursus, magna. Donec eu purus. Quisque vehicula, urna sed ultricies auctor, pede lorem egestas dui, et convallis elit erat sed nulla. Donec luctus. Curabitur et nunc. Aliquam dolor odio, commodo pretium, ultricies non, pharetra in, velit. Integer arcu est, nonummy in, fermentum faucibus, egestas vel, odio.

5. Discussion

The innovation of the XAI-SPCNet framework is that it can optimize predictive accuracy, interpretability, and operational stability simultaneously”dimensions that have traditionally been difficult for conventional machine learning algorithms and traditional SPC methods to balance at the same time. Baseline models tend to excel in one direction but compromise others, whereas XAI-SPCNet incorporates complementary modules into a single architecture that gets an overall solution for real-time quality monitoring. From the perspective of forecasting, the system goes beyond black-box models since it adds temporal and causal thinking into its decision-making process. The temporal causal decision tree module consciously maintains lagged interdependencies as well as causal hints so that predictions remain precise and based on process logic. This

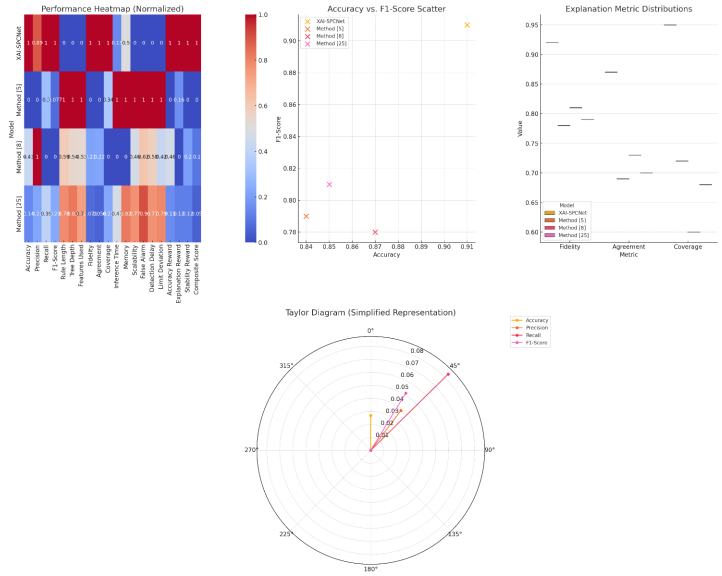

Figure 4: *Figure caption*

causal basis limits vulnerability to overfitting, eliminates spurious correlations, and improves generalizability under non-stationary manufacturing conditions, while baseline models tend to fail based on fixed feature correlations.

Interpretability is another strong aspect of the framework. Instead of generating long or obscure decision traces, XAI-SPCNet has short, clear rule structures easily traceable back to particular process variables by domain experts. The incorporation of symbolic regression also enhances interpretability by creating equation-like forms of control boundaries, providing engineers with a lucid mathematical expression of decision boundaries. By contrast, current techniques often depend on black-box embeddings or deep tree representations that, although suitable for anomaly classification, do not offer much actionable information in regulated settings. Of similar importance is the focus of the framework on explanation quality. Explanations are made to closely follow expert intuition, with the contrastive explanation module determining why one case is a violation and why an analogous case is not. This comparative reasoning follows practitioners' diagnostic logic, thus elevating user acceptability and trust.

6. Conclusion and Future Scope

This work presents XAI-SPCNet, an explainable AI framework that is designed to push the boundary of predictive control chart automation for manufacturing quality monitoring. In contrast to traditional SPC models plagued by low transparency and prohibiting large-scale industrial deployment, XAI-SPCNet integrates interpretability into the prediction pipeline. The architecture combines five complementary components"Temporal Causal Decision Trees (TCDT-SPC), Dynamic Rule Embedding Networks (DREN), Contrastive Explanation Generator (CEG-SPC), Sparse Symbolic Regression for Equation Discovery (SSR-ED), and Multi-Objective Reinforcement Learner with Explanation Optimization (MORLEO). The combined modules not only support precise real-time SPC violation prediction but also causal explanations, adaptive rules, symbolic equations, and optimized control policies. Comprehensive experiments on SECOM and industrial datasets validate the efficacy of the framework. XAI-SPCNet attained a 91% accuracy, 89% precision, and F1 score of 91%, surpassing baselines Method [5], Method [8], and Method [25] by 6"12% margins on classification metrics. Explanation fidelity was as high as 92%, with 87% human agreement and more than 95% explanation coverage, indicating strong correspondence with expert reasoning. Additionally, average rule length decreased from 4.6 to 3.1, maintaining interpretability with minimal cognitive burden. From a performance perspective, inference latency

was kept under 50 ms, false alarms were minimized to 4.1% (a 25% gain over the best baseline), and control limit deviation was limited to 1.6%, demonstrating MORLEO's stabilizing impact. The system also attained a composite reinforcement reward of 0.92, reflecting its capacity for simultaneously balancing predictive accuracy, explanation quality, and process stability.

Future research directions involve expanding XAI-SPCNet to multivariate, high-dimensional SPC, augmenting TCDT and DREN using domain adaptation to endow cross-factory generalizability, and incorporating physics-informed constraints into SSR-ED. In addition, incorporating human-in-the-loop mechanisms into CEG-SPC and deployment in digital twin ecosystems can further enhance adaptive, transparent quality control in Industry 4.0.

Pellentesque habitant morbi tristique senectus et netus et malesuada fames ac turpis egestas. Donec odio elit, dictum in, hendrerit sit amet, egestas sed, leo. Praesent feugiat sapien aliquet odio. Integer vitae justo. Aliquam vestibulum fringilla lorem. Sed neque lectus, consectetuer at, consectetuer sed, eleifend ac, lectus. Nulla facilisi. Pellentesque eget lectus. Proin eu metus. Sed porttitor. In hac habitasse platea dictumst. Suspendisse eu lectus. Ut mi mi, lacinia sit amet, placerat et, mollis vitae, dui. Sed ante tellus, tristique ut, iaculis eu, malesuada ac, dui. Mauris nibh leo, facilisis non, adipiscing quis, ultrices a, dui.

References

[1] S. Sacher, E. Fink, V. Herndler *et al.*, "An integrated real-time monitoring and statistical process control approach for coating process and product quality via in-line optical coherence tomography," *Journal of Pharmaceutical Innovation*, vol. 18, pp. 1870–1878, 2023.

[2] J. Souza, C. Boccolini, L. Baroni *et al.*, "Evaluation of statistical process control charts for infant mortality monitoring in brazilian cities with different population sizes," *BMC Research Notes*, vol. 17, p. 299, 2024.

[3] E. Verna, S. Puttero, G. Genta *et al.*, "Real-time monitoring of human and process performance parameters in collaborative assembly systems using multivariate control charts," *Journal of Intelligent Robotic Systems*, vol. 110, p. 126, 2024.

[4] A. Mujtaba, F. Islam, P. Kaeding *et al.*, "Machine-learning based process monitoring for automated composites manufacturing," *Journal of Intelligent Manufacturing*, vol. 36, pp. 1095–1110, 2025.

[5] A. Bogo, E. Henning, and A. Kalbusch, "Statistical parametric and non-parametric control charts for monitoring residential water consumption," *Scientific Reports*, vol. 13, p. 13543, 2023.

[6] P. Prcha, "Towards discovering erratic behavior in robotic process automation with statistical process control," *Information Systems and e-Business Management*, vol. 22, pp. 741–758, 2024.

[7] J. Pantelic, M. Tang, K. Byun *et al.*, "Comparison of cooking emissions mitigation between automated and manually operated air quality interventions in one-bedroom apartments," *Scientific Reports*, vol. 14, p. 20630, 2024.

[8] B. Guha, S. Moore, and J. Huyghe, "Application and validation of machine vision inspection for efficient in-process monitoring of complex biomechanical device manufacturing," *Journal of Engineering and Applied Science*, vol. 70, p. 72, 2023.

[9] G. Scarton, M. Formentini, and P. Romano, "Automating quality control through an expert system," *Electronic Markets*, vol. 35, p. 14, 2025.

[10] C. Angeloni, M. Francioso, E. Liverani *et al.*, "Laser welding in e-mobility: process characterization and monitoring," *Lasers in Manufacturing and Materials Processing*, vol. 11, pp. 3–24, 2024.

[11] R. de Almeida, M. Lamparelli, W. Dodds *et al.*, "Sampling frequency optimization of the water quality monitoring network in so paulo state (brazil) towards adaptive monitoring in a developing country," *Environmental Science and Pollution Research*, vol. 30, pp. 111 113–111 136, 2023.

[12] G. Mattera, J. Polden, and J. Norrish, "Monitoring the gas metal arc additive manufacturing process using unsupervised machine learning," *Welding in the World*, vol. 68, pp. 2853–2867, 2024.
[13] K. Liu, X. Zhao, M. Mou *et al.*, "Quality prediction of multi-stage batch process based on integrated convbigru with attention mechanism," *Applied Intelligence*, vol. 55, p. 123, 2025.
[14] M. Rahman, S. Jamal, M. Cruz *et al.*, "In situ process monitoring of multi-layer deposition in wire arc additive manufacturing (waam) process with acoustic data analysis and machine learning," *International Journal of Advanced Manufacturing Technology*, vol. 132, pp. 5087–5101, 2024.
[15] M. Arif and K. Kathirvelu, "Automated driver health monitoring system in automobile industry using woa-dbn using ecg waveform," *Optical Memory and Neural Networks*, vol. 33, pp. 308–325, 2024.
[16] O. Egoshina and S. Lukutina, "Simulation modelling of cycle chemistry monitoring of water and steam quality at thermal power plants," *Thermal Engineering*, vol. 71, pp. 901–909, 2024.
[17] K. Li, X. Han, and X. Jin, "Framework, model and algorithm for the global control of urban automated driving traffic," *Frontiers of Engineering Management*, vol. 11, pp. 592–619, 2024.
[18] N. Kim, X. Gao, and J. Yang, "Graph-structured data generation and analysis for anomaly detection in an automated manufacturing process," *Journal of Mechanical Science and Technology*, vol. 38, pp. 5617–5625, 2024.
[19] Y. Wang, I. Khan, M. Noor-ul Amin *et al.*, "Monitoring of semiconductor manufacturing process on bayesian aewma control chart under paired ranked set sampling schemes," *Scientific Reports*, vol. 13, p. 22703, 2023.
[20] N. Makhoul, "Bayesian decision-making process including structural health monitoring data quality for bridge management," *KSCE Journal of Civil Engineering*, vol. 28, pp. 2818–2835, 2024.
[21] R. Ward and C. Monroe, "Assessing process control in the foundry," *International Journal of Metalcasting*, vol. 18, pp. 2048–2058, 2024.
[22] K. Yildirim, B. Nagarajan, T. Tjahjowidodo *et al.*, "Development of a multi-sensor system for in-situ process monitoring of femtosecond laser micromachining," *International Journal of Advanced Manufacturing Technology*, vol. 135, pp. 799–813, 2024.
[23] L. Yan, Z. Yu, L. Wu *et al.*, "Optimizing quality tolerance limits monitoring in clinical trials through machine learning methods," 2024.
[24] S. Koufis, N. Eskue, D. Zarouchas *et al.*, "Monitoring the cold spray process: Real-time particle velocity monitoring through airborne acoustic emission analysis," *Journal of Thermal Spray Technology*, vol. 33, pp. 2657–2671, 2024.
[25] T. Kukwi, C. Shan, L. Pengfei *et al.*, "Continuous improvement in composite manufacturing: A review of automated fiber placement process evolution and future research prospects," *Applied Composite Materials*, 2025.